VNIR Push-Broom HSI Imager ATH1100

Features

- Spectral Range: 390~1000nm
- Hyperspectral Resolution: Better than 1.5 nm
- Built-in push-broom imaging
- Spectral Pathway: Holographic transmission grating
- Maximum Field of View: 31.7° (customizable)
- Minimum Instantaneous FOV: 0.7 mrad
- Superior imaging performance
- Powerful image compression algorithm
- Compact design: 77mm x 285mm x 105mm
- Weight: <1000g

Application

- Geology and mineral resource：Oil、Mining、Energy
- Agriculture: crop growth and Seed testing
- Environmental Monitoring： Forest pest and disease monitoring and fire prevention
- Environmental Monitoring：Coastal and marine environment
- Environmental Monitoring： Grassland productivity and monitoring
- Environmental Monitoring：Lake and watershed
- Scientific Research：Remote sensor
- Scientific Research：Meteorological research
- Mining & Environmental Analysis
- Environmental Monitoring： Water Bodies Monitoring & Water Stress
- Food Safety： Agricultural and livestock product quality testing
- Public Safety：Military, Defense, Homeland security
- Environmental Science：Disaster prevention and mitigation

Description

The ATH1100 is a compact and lightweight mini hyperspectral imager suitable for both indoor and outdoor scenes. Beyond its small size and light weight, the ATH1100 features high spatial resolution, high spectral resolution, and a broad imaging range. It consists of two parts: an imaging lens and a hyperspectral imager. The hyperspectral imager, based on transmission grating technology, exhibits excellent aberration characteristics.

The ATH1100 uses a high-performance CCD imaging device with 1920×1200 pixels, producing clear images with minimal noise. The ATH1100 model is a conventional straight-tube hyperspectral imager, ideal for multi-rotor drones.

The ATH1100 can be used for real-time spectral information measurement of objects such as plants, water bodies, and soil, obtaining spectral images. By analyzing these spectral images, relationships can be established with the physical and chemical properties of plants, aiding in plant classification and growth condition studies. The entire system is compactly designed with a high spectral resolution in the main hyperspectral imager unit. Using a built-in push-broom imaging method, it can function as an independent measurement system or be mounted on a drone for aerial remote sensing operations.

Model	Features
ATH1100	390~1000nm，1920X1200pixels, built-in push-broom
ATH1100-17	900~1700nm，640X512pixels, built-in push-broom

1.Parameter

Serial No.	Specifications	ATH1100	ATH1100-17
1	Spectral Range	390~1000 nm	900~1700 nm
2	Spectral Resolution (FWHM)	No Binning: Better than 1.3 nm 4X4 binning: 1.7 nm	No Binning: Better than 1.3 nm 4X4 binning: 2.2 nm
3	Sampling Interval	0.31 nm	0.29 nm
4	F-number (F/#)	F/2.4	F/2.6
5	Detector	CMOS	CMOS
6	Interface	USB3.0	USB3.0
7	Power Consumption	USB powered, 3.4 W	USB powered, 4.5 W
8	Detector Size	11.3 mm × 7.03 mm	9.6 mm × 7.7 mm
9	Detector Resolution	1920 × 1200	640 × 512
10	Pixel Size	5.86μm x 5.86μm	15μm x15μm
11	Bit Depth	12 bits	14 bits
12	SNR	45 dB	43 dB
13	Dynamic range	73 dB	60 dB
14	Slit Width	15 μm, 25μm, etc., customizable	15 μm，25μmetc., customizable
15	Binning Mode	4×4 / 2×4	4×4 / 2×4
16	Spatial Bands	1200	512
17	Spectral Bands	1920	640
18	FOV	11.5°@f=35 mm	12.5°@f=35 mm
19	IFOV	0.17mrad@f=35 mm	0.43mrad@f=35 mm
20	Frame Rate	164 fps	120 fps
21	Focal Length	25 mm，35mm customizable	25 mm，35mm customizable

22	Dimensions	77mm x285mm x105mm	80mm x275mm x104mm
23	Spatial Resolution	0.016 m (@35mm, 100m flying altitude)	0.015 m (@35mm, 100m flying altitude)
24	Weight	Less than 545 g	Less than 680 g
25	Working Temperature	-20℃~50℃	-20℃~50℃
26	Storage Temperature	-30℃~70℃	-30℃~70℃

*1: This value was measured under 4X4 binning conditions. Binning operations can enhance the signal-to-noise ratio.

2. ATH1100 Imaging Test

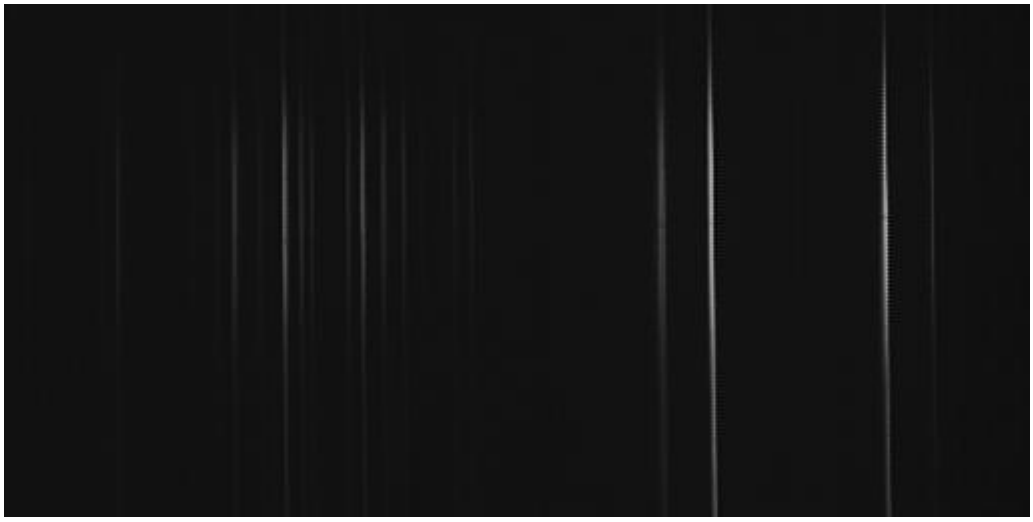

Figure 2: Spectral image of a mercury lamp taken by the ATH1100, with a resolution better than 1.3 nm @ 578 nm (without binning).

3. ATH1100 Image and dimensional diagram

Figure 3: ATH1100 Model Hyperspectral Imager

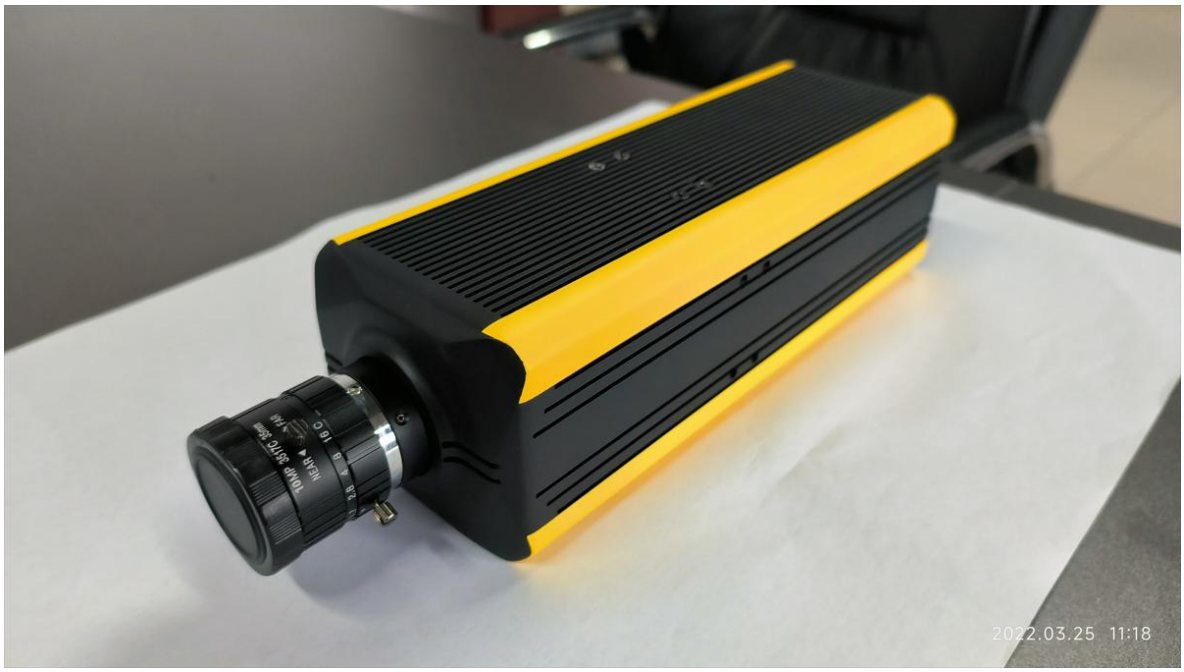

Figure 4: ATH1100 Model Hyperspectral Imager

Figure 5: Flight results of the ATH9100 Drone Hyperspectral Imager (EVI Reversion Index)

4

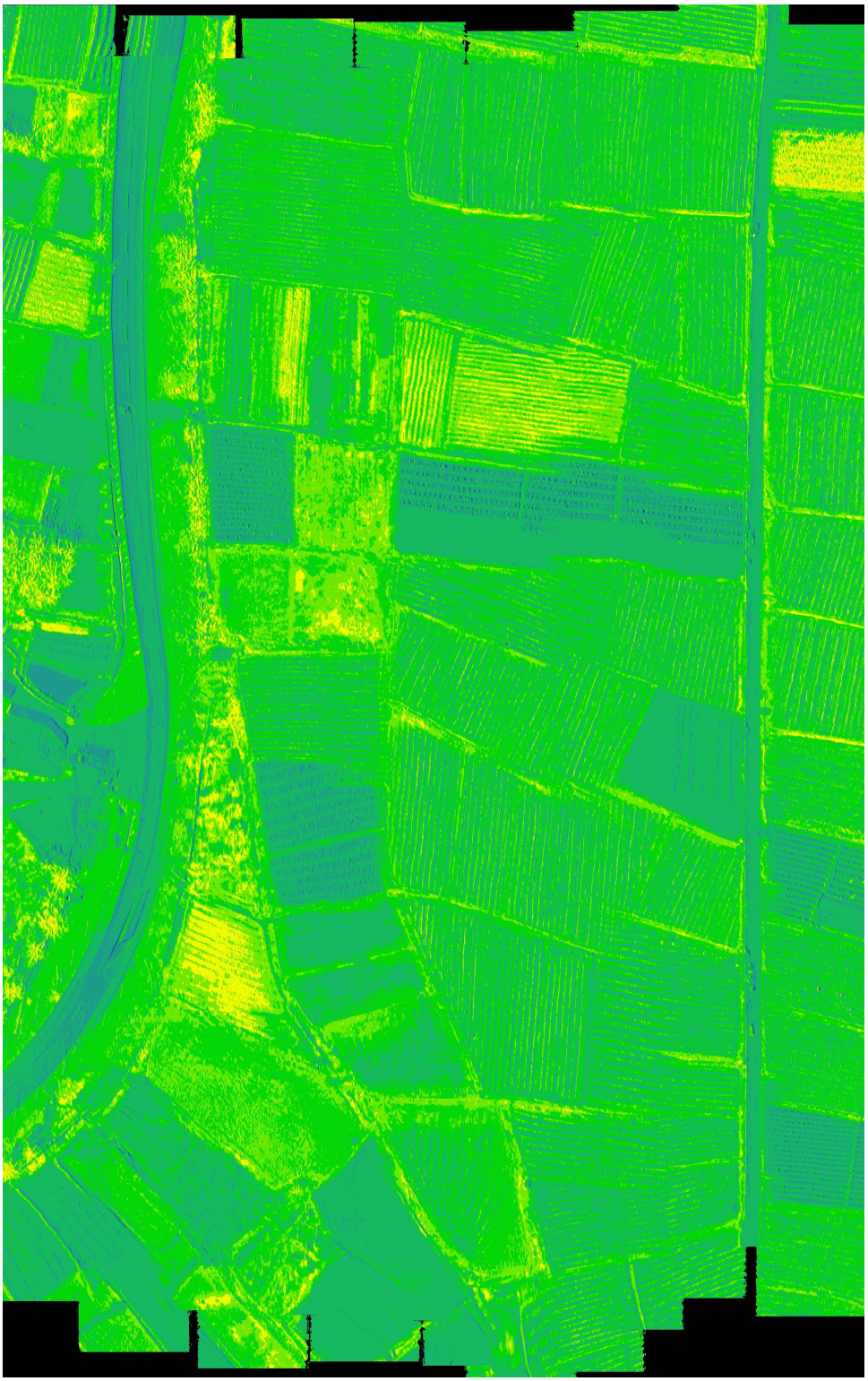

Figure 6: Flight results of the ATH9100 Drone Hyperspectral Imager (NDVI Reversion Index)

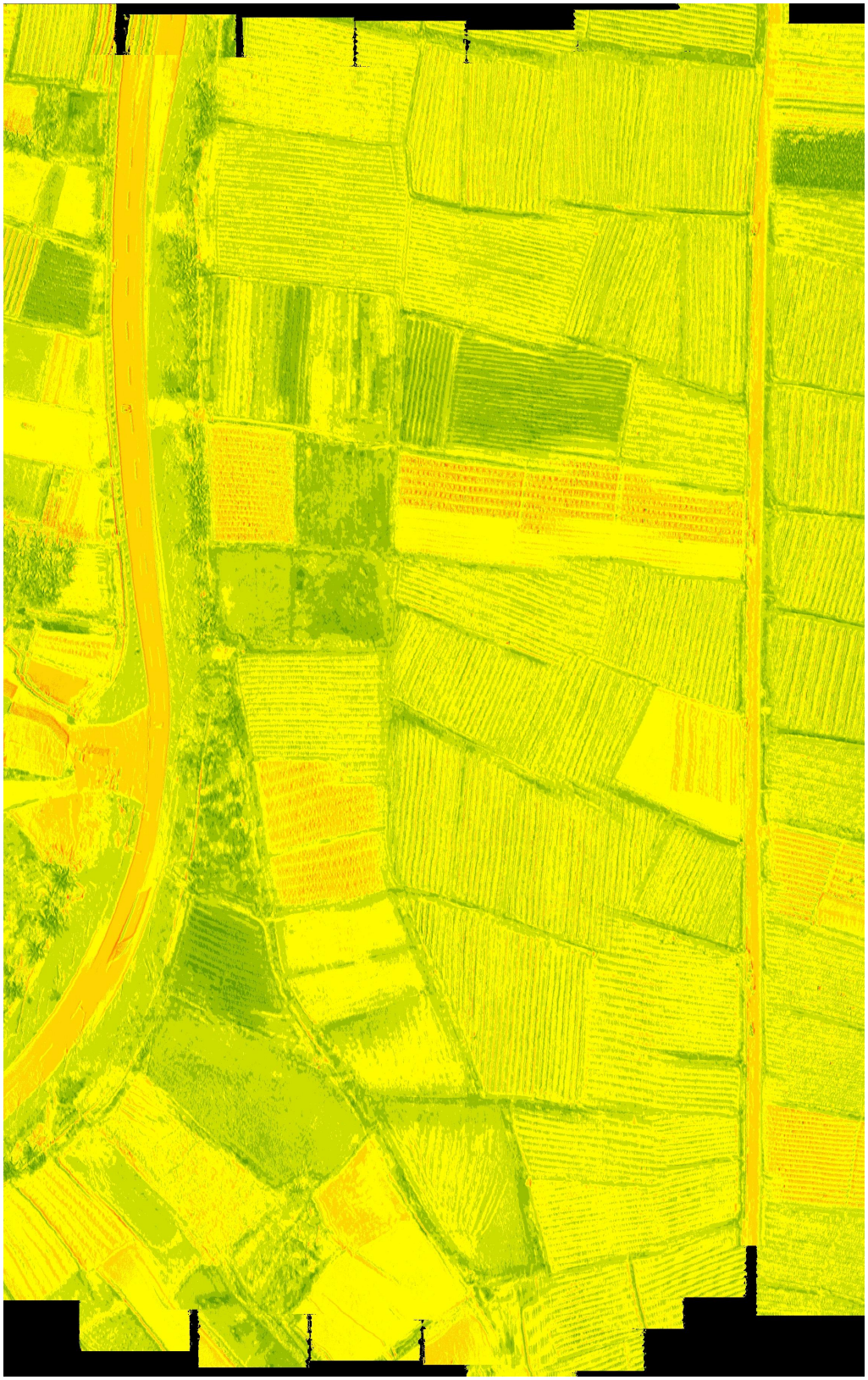

Figure 7: Flight results of the ATH9100 Drone Hyperspectral Imager (ARVI Reversion Index)

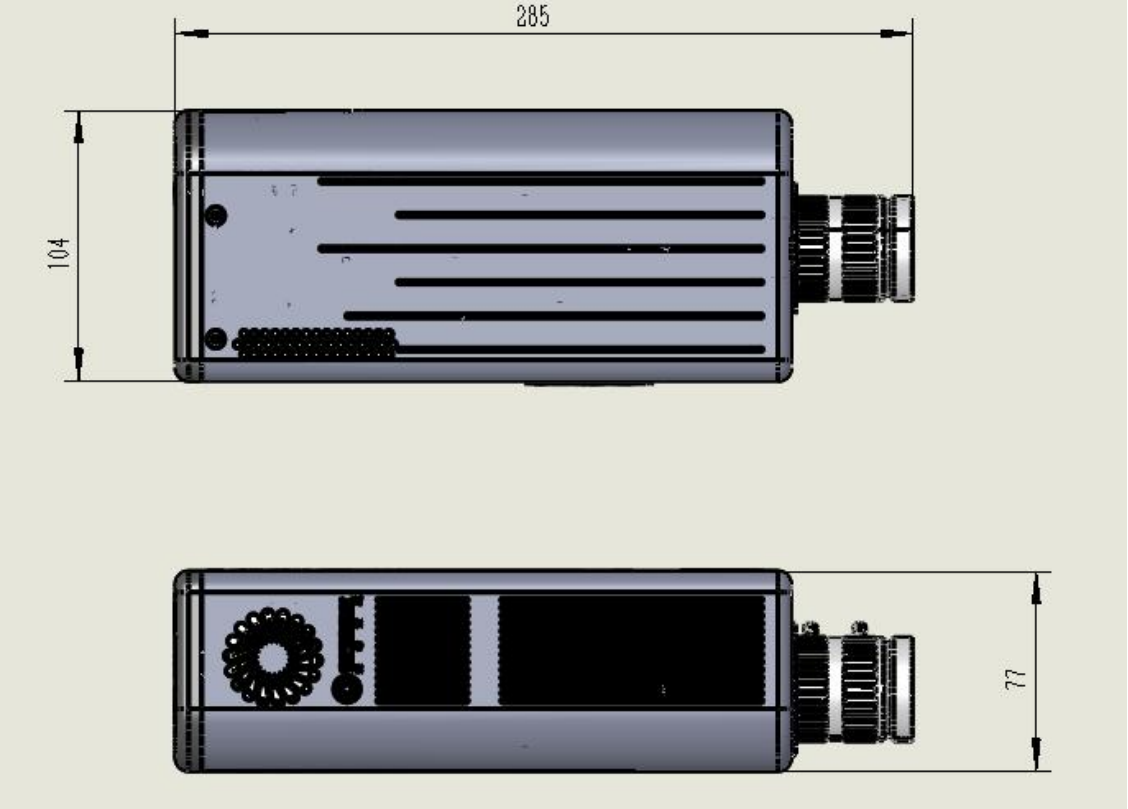

Figure 8: External dimensions of the ATH1100 Hyperspectral Imager

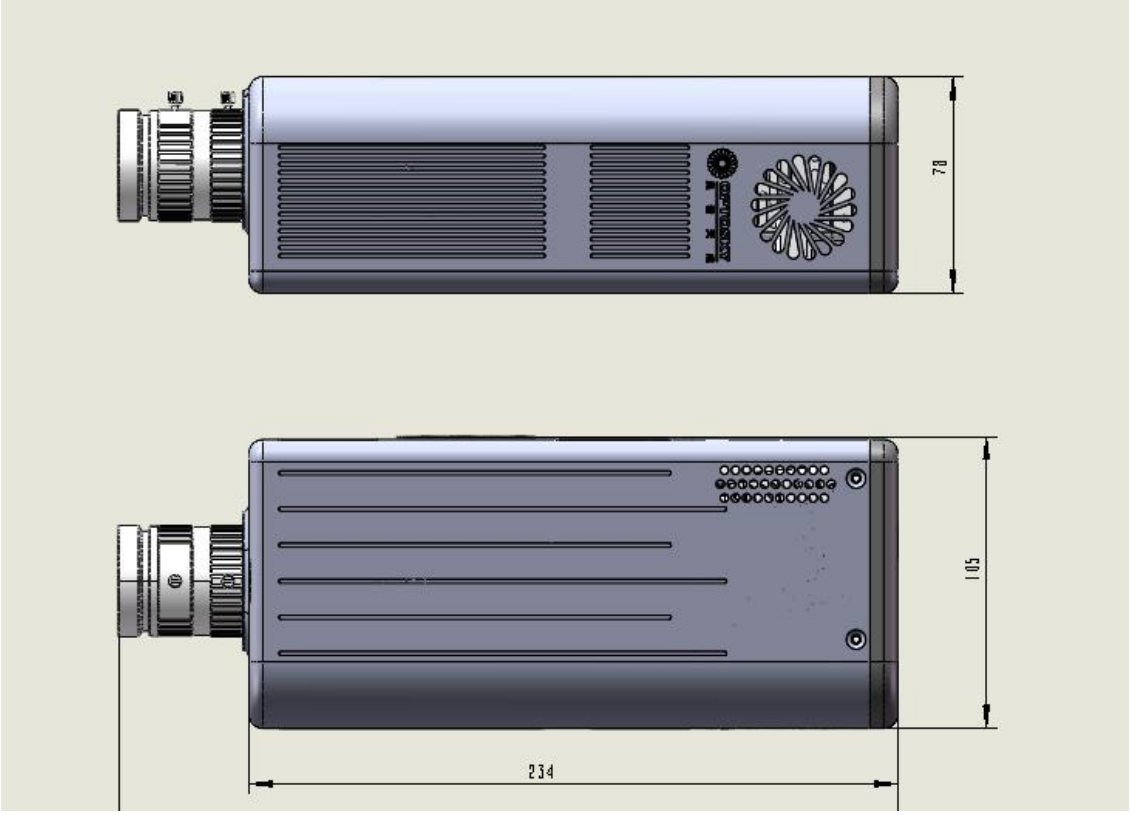

Figure 9: External Dimensions of ATH1100-17 Hyperspectral Imager

4. Application Cases

Figure 10: Drone Mounting Experiment

Figure 11: Field Experiment Scene

1

Figure 12: Field Experiment Scene 2

Figure 13: Field Experiment Scene 3

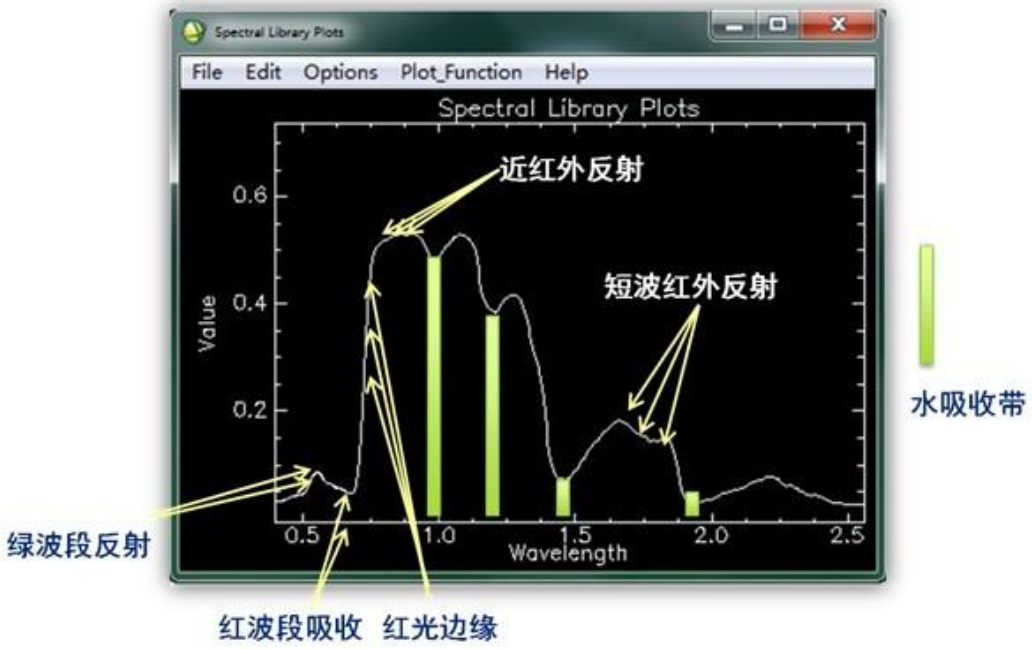

Figure 14: Spectral image of green plants measured by the hyperspectral imager

4.1 Application in Mineral Exploration

Spectral remote sensing technology, which evolved from multispectral remote sensing technologies represented by Landsat, took shape in the mid-1980s (Goets et al., 1985; Tong Qingxi et al., 2006). Due to its high spectral resolution and the integration of imaging and spectral data, hyperspectral remote sensing technology can finely detect and analyze the composition of surface rocks and minerals on a large spatial scale. It not only provides macroscopic images of the ground but also identifies the types and abundance of minerals in geological formations at the pixel level, and even the chemical composition of some minerals (Wang Runsheng et al., 2010).

In recent years, the continuous development of hardware and data processing methods and software related to imaging spectrometers has accelerated the application of hyperspectral remote sensing technology in geological surveys. From large metallogenic belts to medium-sized ore fields, hyperspectral remote sensing technology has played a crucial role in geological mapping, delineating hydrothermal alteration zones, and identifying and delineating mineralization anomaly areas (e.g., Bierwirth et al., 2002; Lian Changyun et al., 2005; Kruse et al., 2006; Cudahy et al., 2007; Wang Runsheng et al., 2010; Liu Dezhang et al., 2011; Yan Baikun et al., 2014; Yang Zian et al., 2015; Graham et al., 2017). With the deeper integration of metallogenic system theories (Wyborn et al., 1994) into mineral exploration practices, thematic mineral mapping at the scale of large mineralization zones and belts will provide key regional compositional information for predictive mineral exploration.

The spectral wavelength ranges used for mineral mapping include visible light (400-700 nm), near-infrared (700-1000 nm), shortwave infrared (1000-2500 nm), and thermal infrared (7000-15000 nm). Currently, the shortwave infrared region (1000-2500 nm) is the most widely used in mining applications. This is because the frequencies within this wavelength range are close to the overtones and combination tones of the vibrations of chemical bonds in the mineral lattice, allowing the observation of water-bearing or OH-bearing minerals (mainly phyllosilicates and clays) as well as certain sulfates and carbonates.

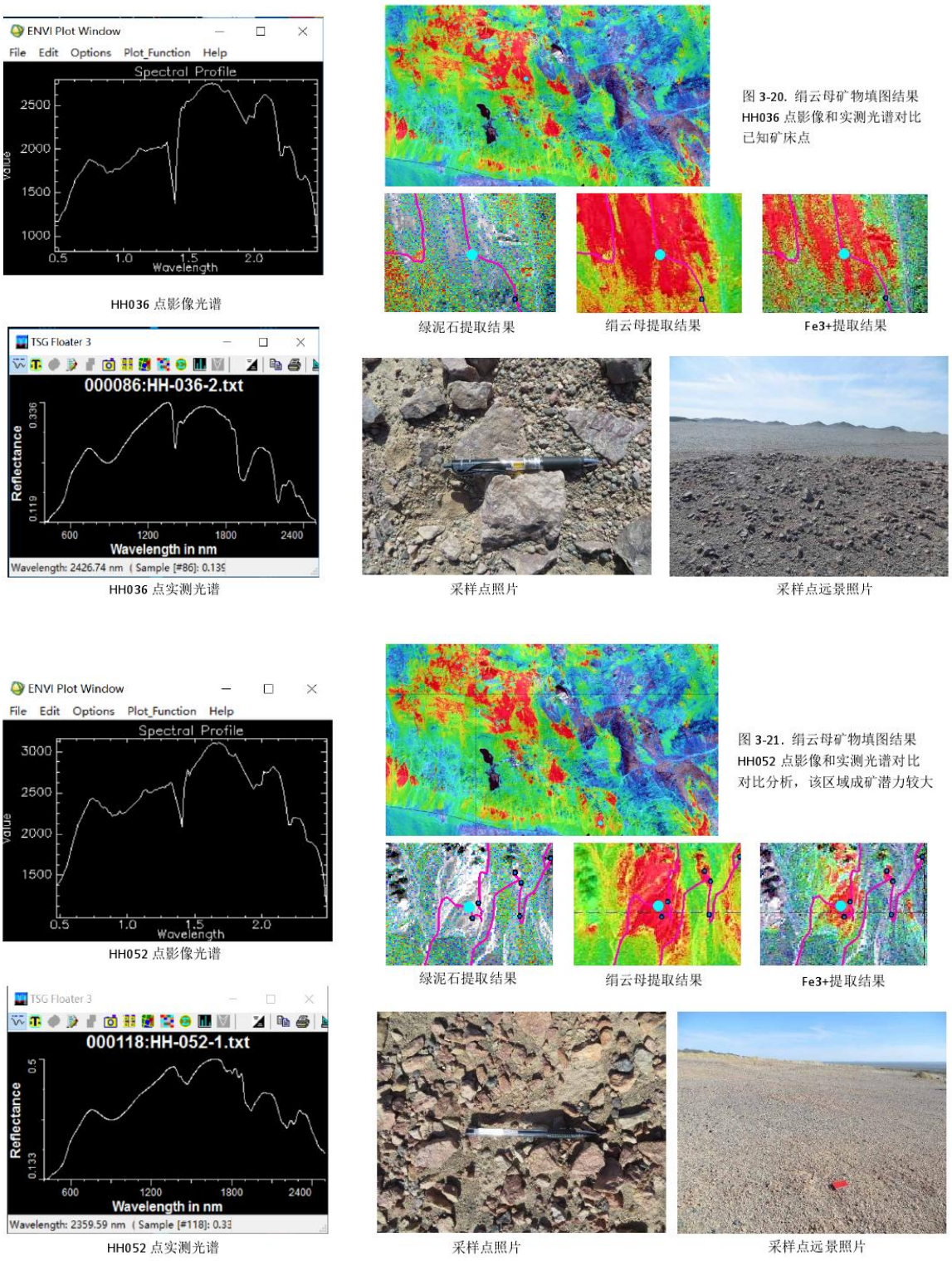

Figure 15: Application of Hyperspectral Imager in Mineral Exploration

Soil salinization is a significant ecological and environmental issue in arid and semi-arid regions. The consequences of soil salinization, such as soil compaction, decreased fertility, pH imbalance, and land degradation, severely restrict agricultural development in China and impact the country's sustainable development strategy. Remote sensing technology,

with its large scale, broad scope, timeliness, and cost-effectiveness, complements traditional methods of monitoring soil salinization. It offers a new approach for the quantitative monitoring of soil salinization phenomena.

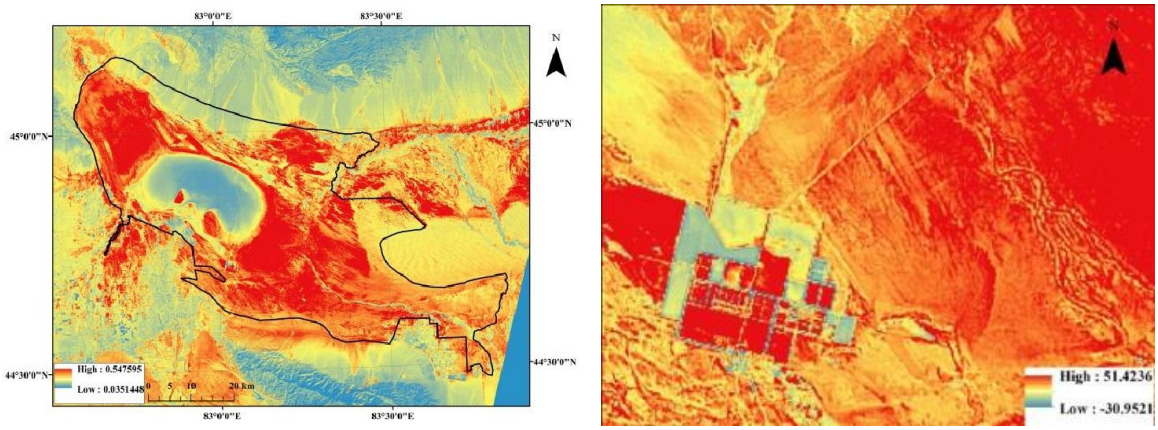

Figure 16: Surrounding Area of a Salt Field

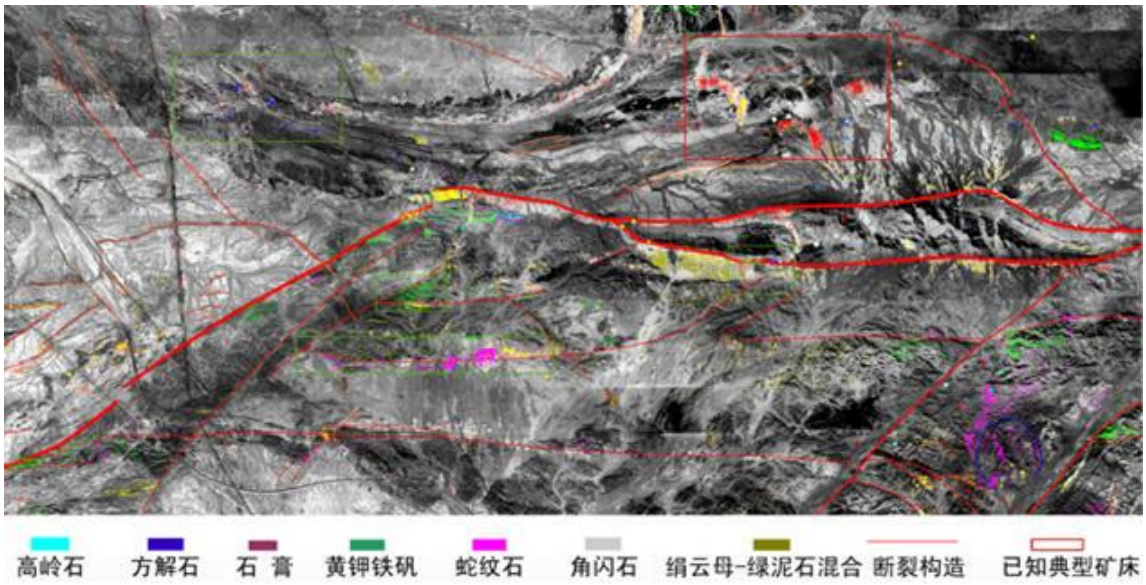

Figure 17: Measurement Map of a Mining Site

4.2 Application in Vegetation Growth Monitoring

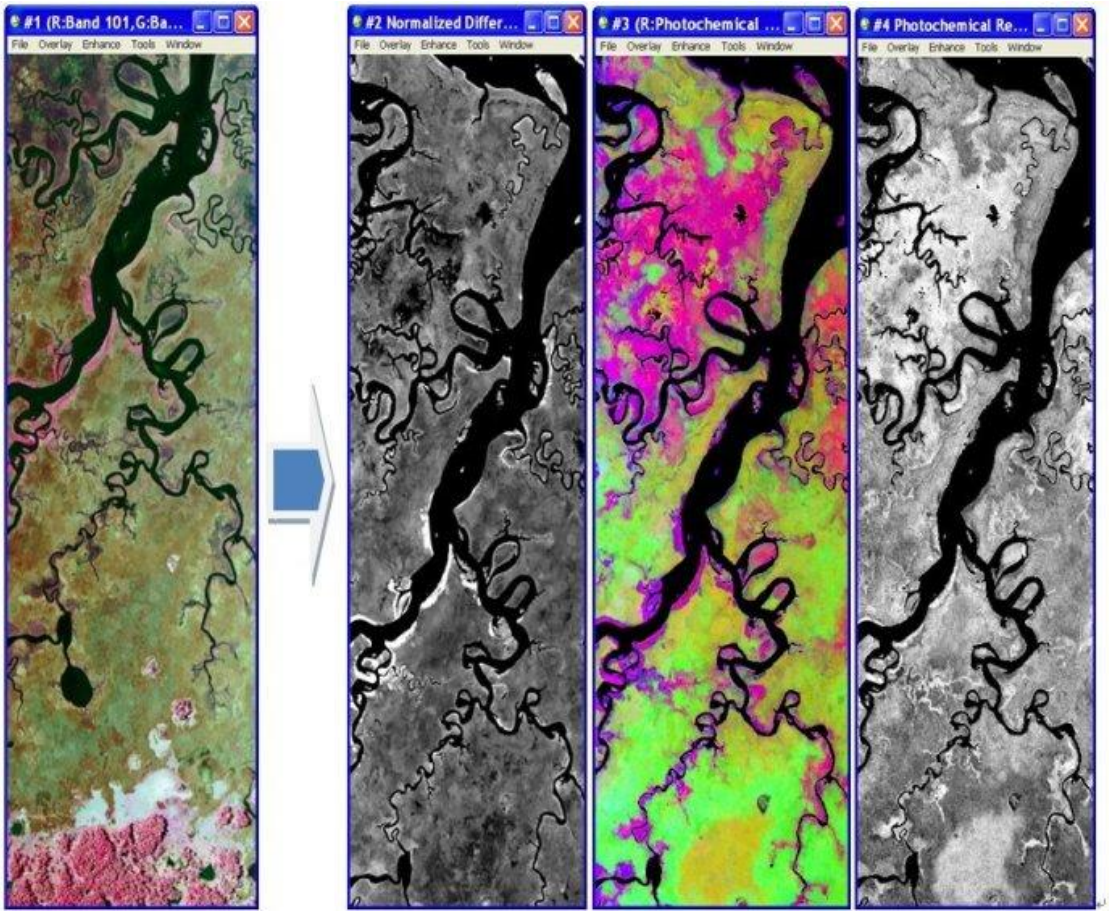

Figure 18: Hyperspectral Imaging of Vegetation Growth

4.3 Application: Forest Health Monitoring

Used for Pest Monitoring and Forest Resource Assessment

Principle: Vegetation health is related to factors such as greenness index, leaf area index, leaf water content, and light use efficiency.

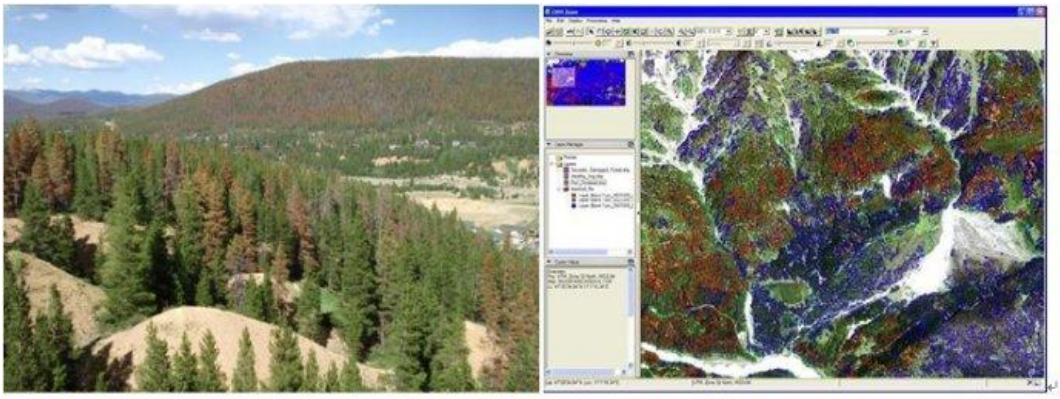

Figure 19: Hyperspectral Imaging Study of the Health of Masson Pine

4.4 Forest Fire Prevention Application

Analysis of Fire Susceptibility and Identification of Fire Ranges and Ignition Points
Principle: The likelihood of vegetation ignition is related to factors such as greenness index, canopy water content, drought conditions, and carbon decay caused by non-photosynthetic vegetation.

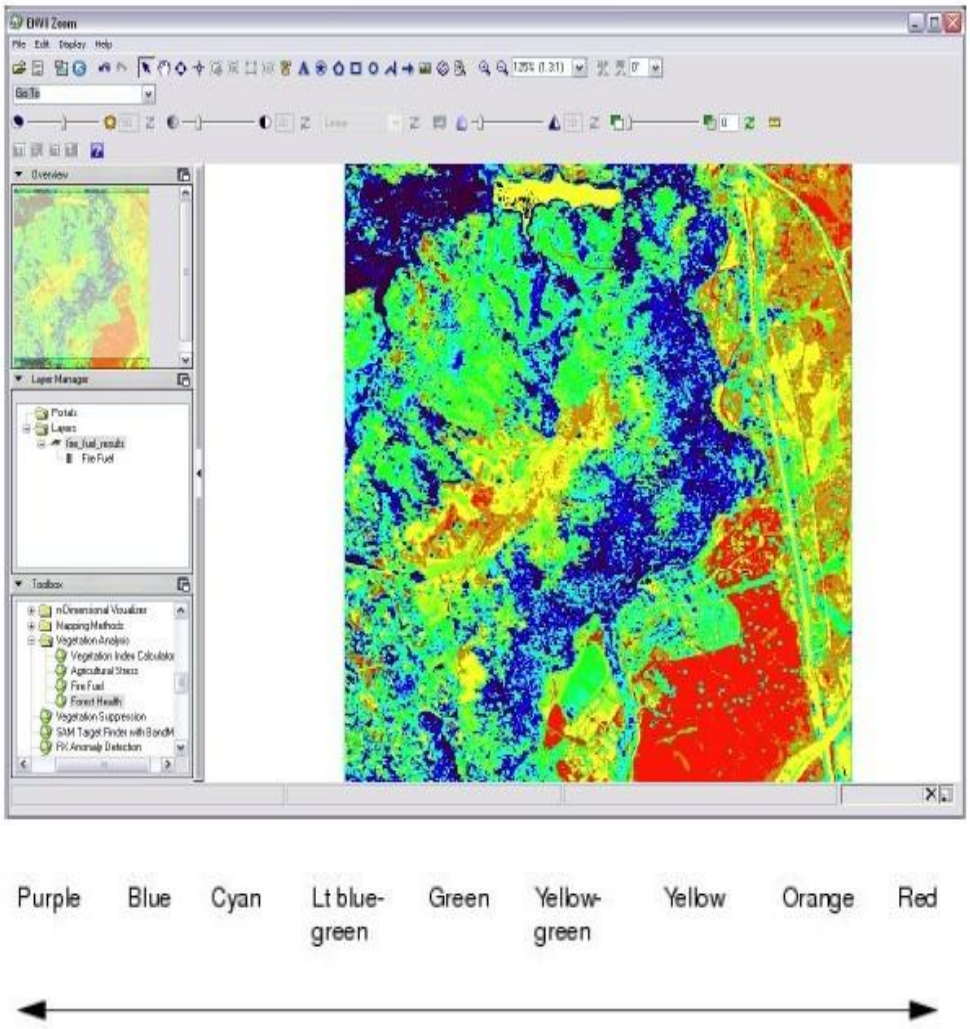

Figure 20: Application of Hyperspectral Imaging in Forest Fire Prevention

4.5 Medical Microscopic Imaging Spectroscopy Application

Application Goal: Intraoperative Online Detection and Navigation Positioning for Tumor Surgery.

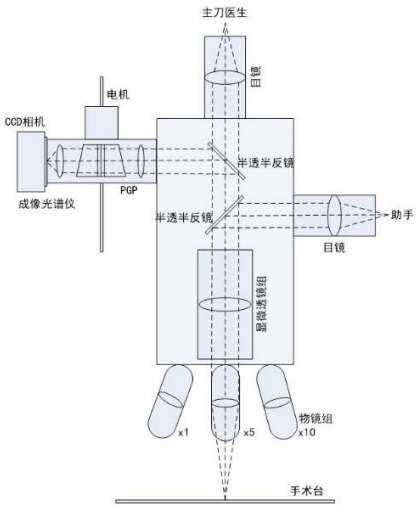

Figure 21: Schematic Diagram of the Optical Path for Medical Microscopic Imaging Spectrometer.

The diagram shows the principle schematic of the medical microscopic imaging spectrometer. The target on the operating table, after passing through the objective lens and the microscopic lens group, is divided into three paths: one path is for the chief surgeon's visual observation, another for the assistant's visual observation, and the third path is detected by the imaging spectrometer. The imaging spectrometer, driven by a motor, performs spatial scanning of the target to obtain the imaging spectral information. After data analysis and image processing, the information is displayed on a monitor for the doctors.

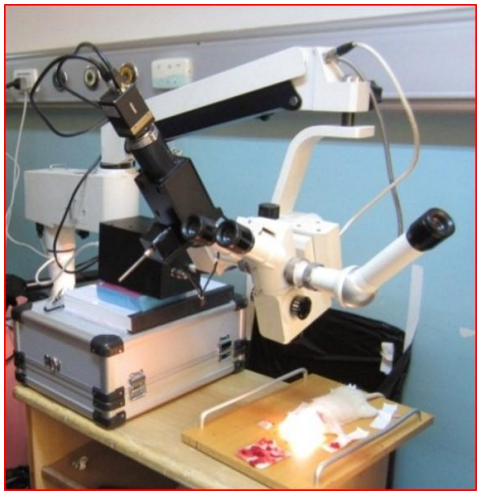

Figure 22: Actual Image of Medical Microscopic Imaging Spectrometer.

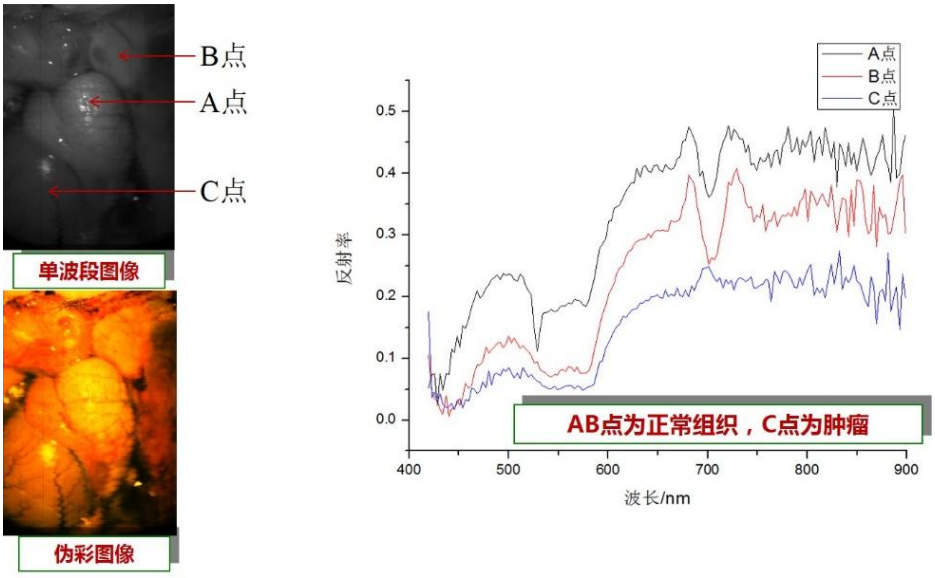

Figure 23: Data of Medical Microscopic Imaging Spectrometer.

4.6 Airborne Imaging Spectroscopy Application

Application Goal：Airborne Remote Sensing

Application Brief: The diagram shows an airborne imaging spectrometer based on SpecVIEW-VIS, composed of SpecVIEW-VIS, a stabilization platform, and a POS module. Figures 20 and 21 show data acquired during a flight over Jingmen, Hubei in December 2014. Figure 20 presents a false-color image after geometric correction, flight strip stitching, and radiometric correction. Figure 21 shows the spectral curve of typical ground objects.

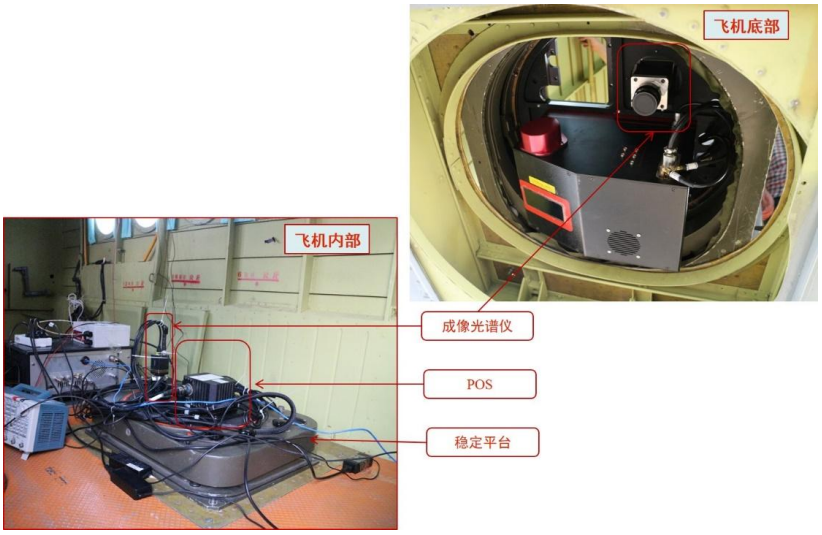

Figure 24: Airborne Remote Sensing Application

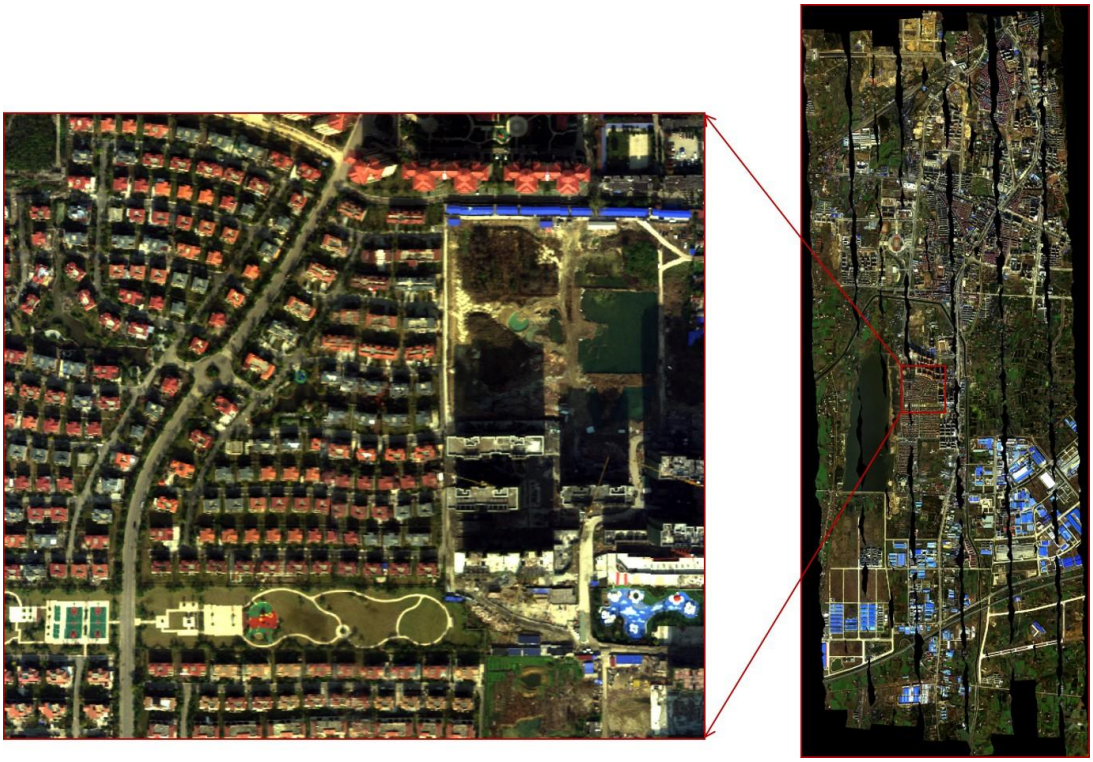

Figure 25: Airborne Application Data — False Color Image

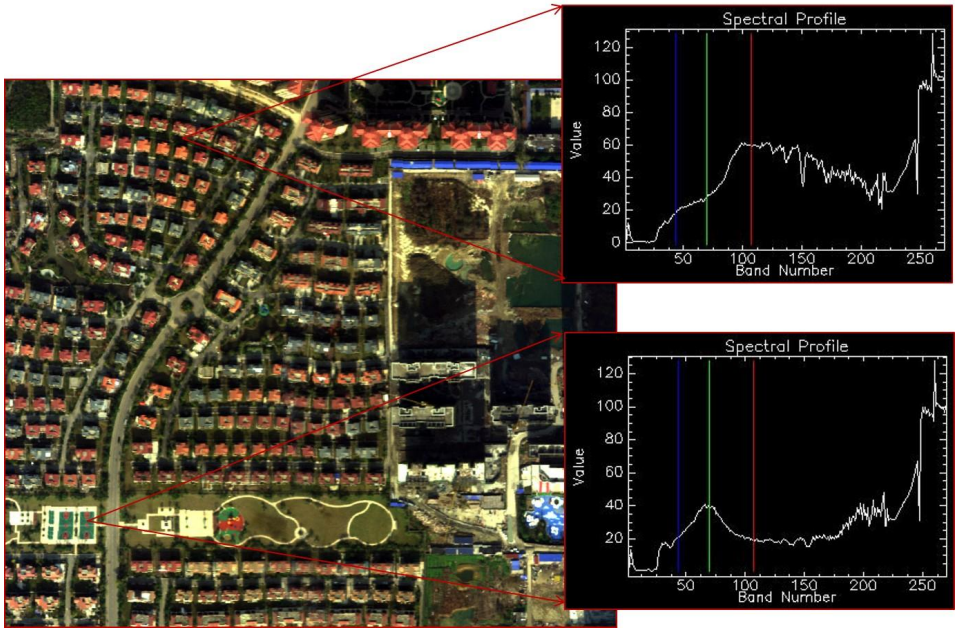

Figure 26: Airborne Application Data — Spectral Curve

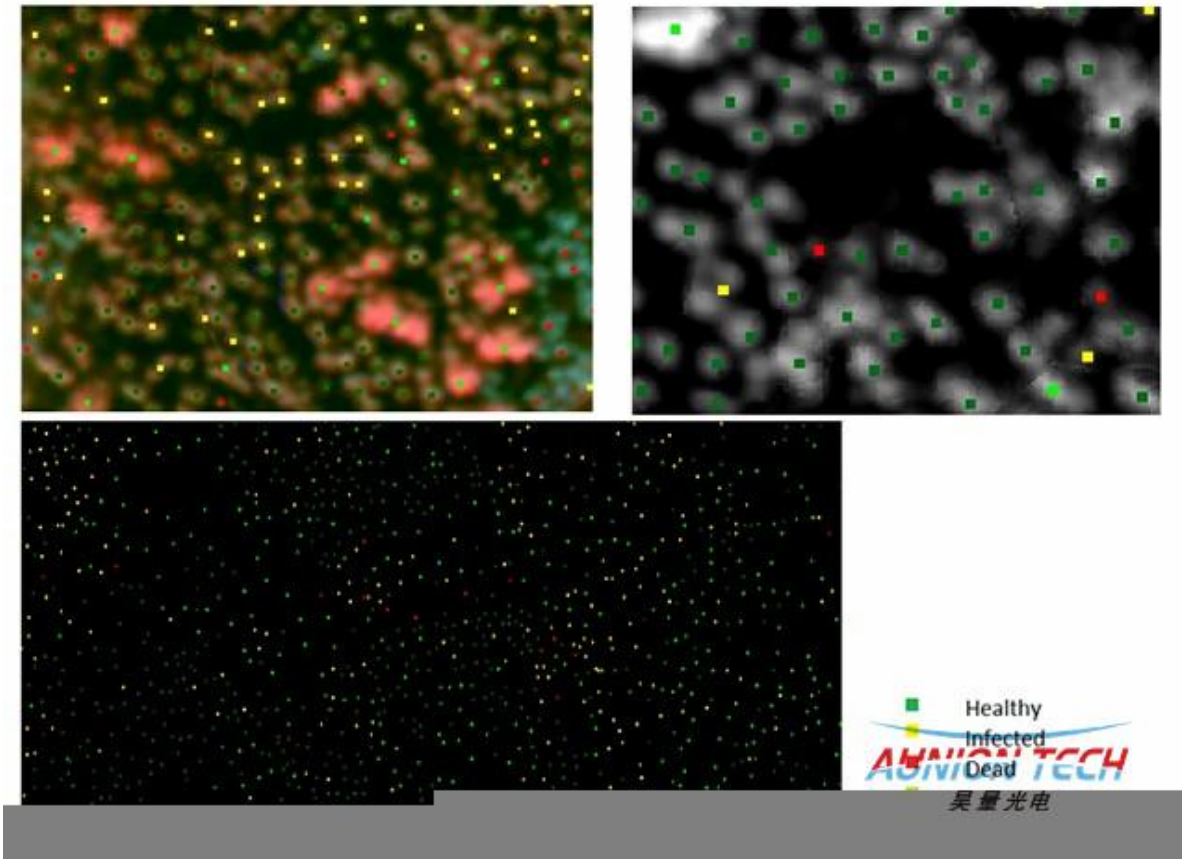

Figure 27: Forest Remote Sensing, Airborne Hyperspectral Observation of Forest Pests and Diseases

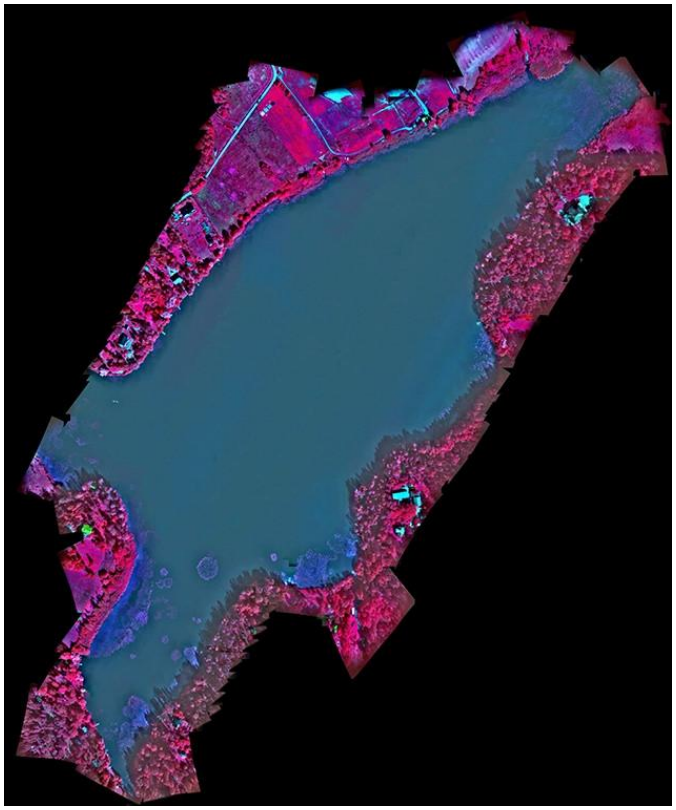

Figure 28: Water Body Detection (Study of Lake Plankton, Algae, and Vegetation)